Flexible Robot Manipulators and Grippers: Relatives of Elephant Trunks and Squid Tentacles

J.F. Wilson[1], D. Li[2], Z. Chen[3], and R.T. George, Jr.[1]

[1]School of Engineering, Duke University, Durham, N.C. 27706, U.S.A.
[2]Tsinghua University, Beijing, China
[3]Department of Electrical Engineering, North Carolina State University, Raleigh, N.C. 27695

Abstract. Elephants and squids have continuously flexible appendages that are well adapted for manipulating and gripping. In this paper we briefly review the overall structural forms and motions of elephant trunks and squid tentacles. We then discuss how we incorporated some of their biological characteristics in the design of a flexible arm manipulator with open loop control (Part 1) and in the design of a flexible, two-fingered gripper with closed loop control (Part 2).

Introduction

Both elephant trunks and squid tentacles are hydrostatic structures; that is, these appendages maintain constant volume as selected muscle groups surrounding this volume contract to achieve particular motions. Cross sections of a trunk and tentacle are depicted in Fig. 1a and Fig. 1b. In both structures, uniform contraction of the longitudinal muscles effects uniform shortening, contraction of longitudinal muscles along one side effects bend-bending, contraction of both circumferential and radial muscles effects elongation, and contraction of the right or left-handed helical muscles leads to respective rotations of the appendage about the longitudinal axis. For detailed discussions of elephant trunk morphology see Wilson et al (1989), and for squid tentacle morphology see Kier and Smith (1985).

P. Dario et al. (eds.), *Robots and Biological Systems: Towards a New Bionics?*

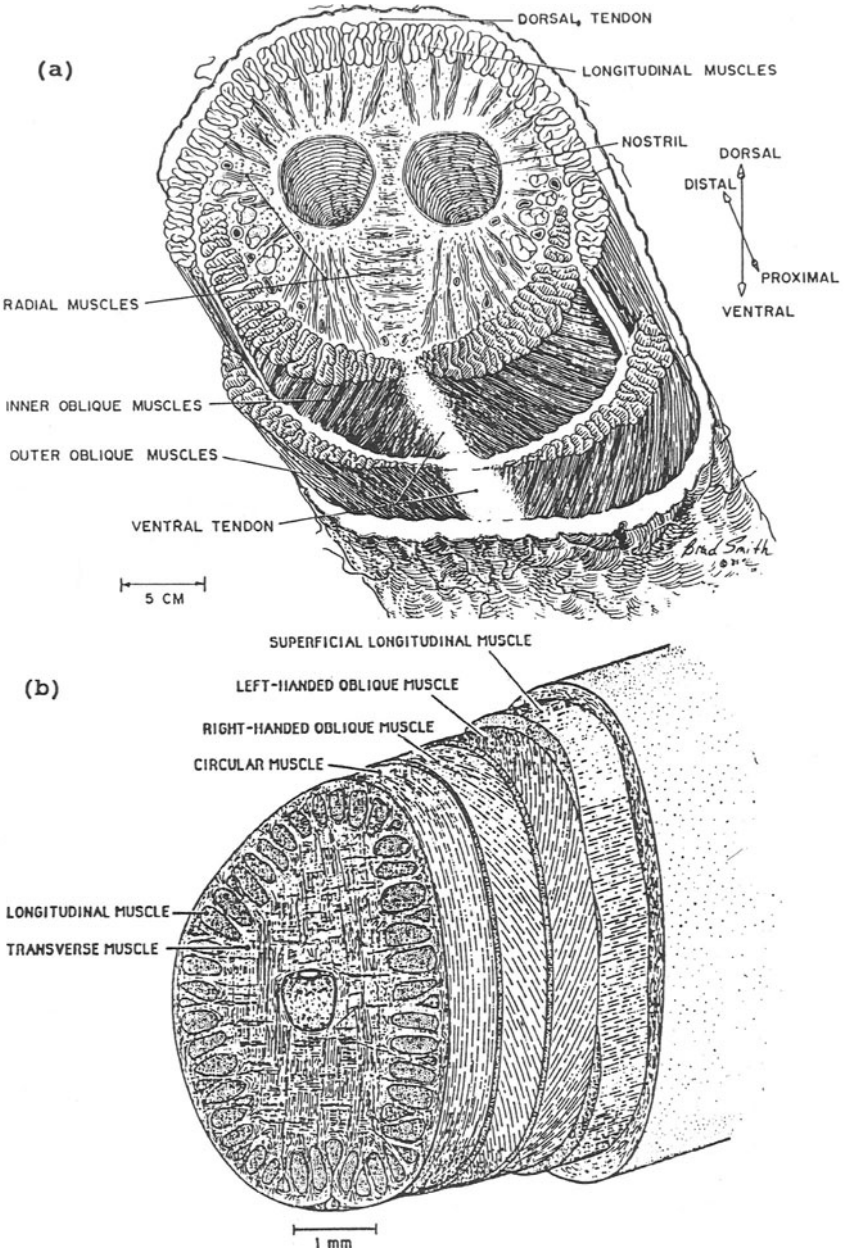

Fig. 1 Cross sections of the muscle structure for:
(a) Trunk of a mature female Asian elephant (drawing by Brad Smith);
(b) Tentacle of a squid, Loligo pealei (adapted from Kier and Smith, 1985).

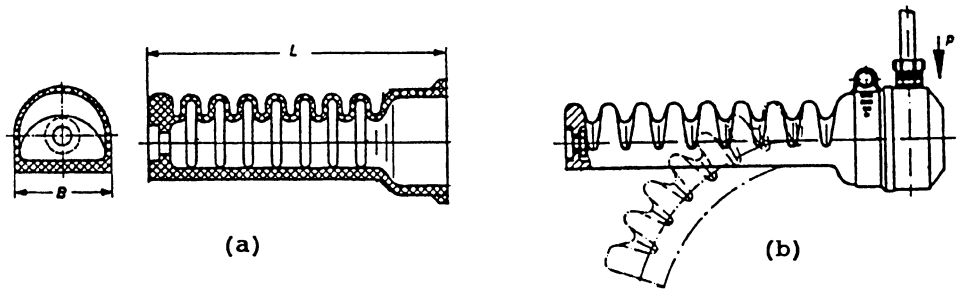

ELEMENT TYPE	DIMENSIONS (mm)	
	B	L
A-1, A-2	40	130
B-1, B-2	28	92
C-1, C-2	20	65

Fig. 2 Polyurethane elements (Simrit Corp., Arlington Heights, IL): (a) unpressurized, (b) pressurized.

Orthotropic, polyurethane tubes that bend when pressurized are depicted in Fig. 2. Placed end-to-end, such elements may simulate the actions of the elephant trunk and the squid tentacle, as discussed by Palaniappan (1985), Ghattas (1988), Wilson and Snyder (1988), Wilson and Mahajan (1989), and Snyder and Wilson (1989). In addition, end effectors for such arms may be configured of such flexible tubes in parallel to form gripping fingers. Although there appears to be no published results on such flexible, pneumatically driven fingers, there are many excellent articles on the mechanics and control of rigid-linked grippers: the especially thorough reviews of the literature by Dario and Buttazzo (1987), Iberall (1987), Li and Sastry (1987), and Nguyen (1989); the recent research of Backé (1986), Kerr and Roth (1986), Kumar and Waldron (1987), and Lee (1988); and the earlier works of Cutkowsky (1984), Datseris and Palm (1984), Hanafusa and Asada (1977), Jacobson et al (1984), Salisbury and Craig (1982), and Wilson (1984a, 1984b).

In the present simulations of arm and finger action, we use the general type of commercially available tube element depicted in Fig. 2a and the three element geometries A, B, C whose overall dimensions are given in the table insert of that figure. These tube elements have a convoluted bellows section for part of the circumference and a flat side that contains its neutral axis of bending. Since the center of pressure on the rigid end caps is offset from the neutral axis of bending, cantilevered elements bend as shown in Fig. 2b when subjected to internal pressure.

In the design of pressure tube systems for robotic applications, it is important to know the mechanical behavior of an individual element under various loading conditions. For the tube element shown in Fig. 2, the measured results are shown in Figs. 3-5. The type of experiment and its variables such as loading

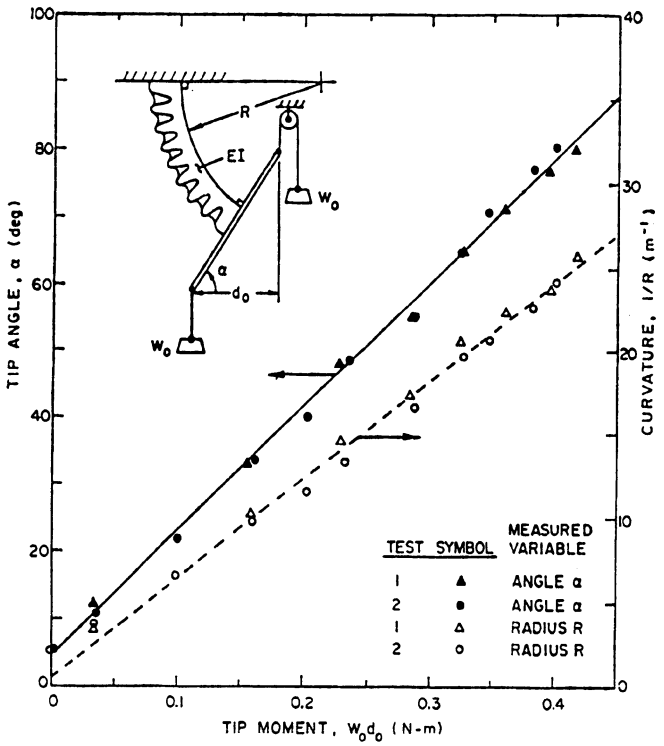

Fig. 3 Elastic behavior of polyurethane element B of Fig. 2, in response to a moment applied to the tip; (from Snyder and Wilson, 1990, and reprinted with permission of ASME).

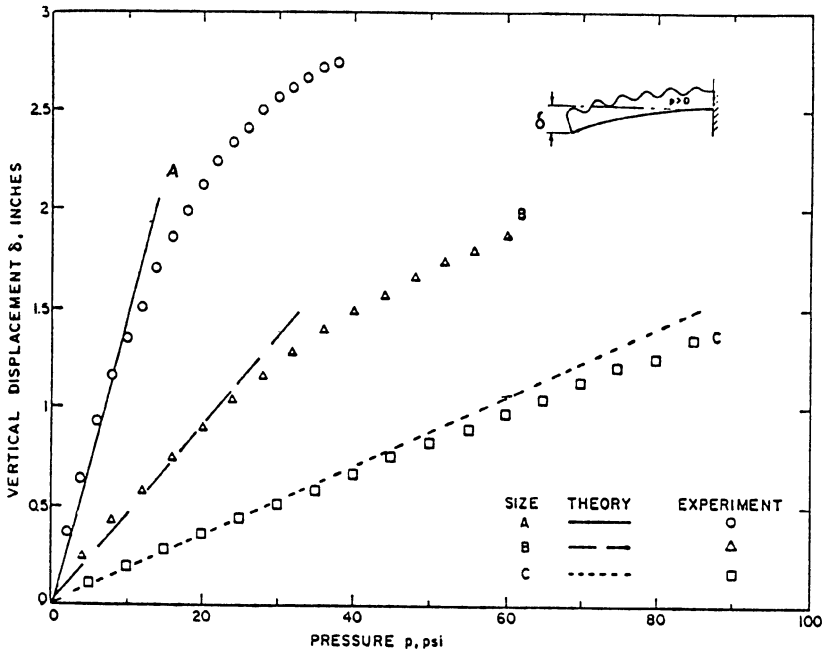

Fig. 4 Transverse tip displacement of polyurethane elements A, B and C under internal pressure only.

and deflection are defined in the inserts of these figures. Thus Fig. 3 shows, for element type B, that the tip angle α and its curvature 1/R both vary linearly with the applied uniform moment at its tip. Figure 4 shows that elements without a transverse tip load have a linear range of transverse tip deflection with internal pressure. Figure 5 shows the transverse tip load F re-required to supress the transverse tip deflection.

Our main objective in this paper is to show through experiments that combinations of such tubes, with proper pressure controls, may be used in applications involving manipulation. In Part I we discuss experiments on a simulated elephant trunk lifting a payload: a simulation comprised of several tubes combined in series, with open loop pressure control, and used in pick-and-place scenarios. In Part II we discuss experiments on a simulated pair of squid tentacles: a simulation comprised of two tubes combined in parallel, with closed loop pressure control, and used to achieve a constant gripping force on an object being manipulated within its grasp.

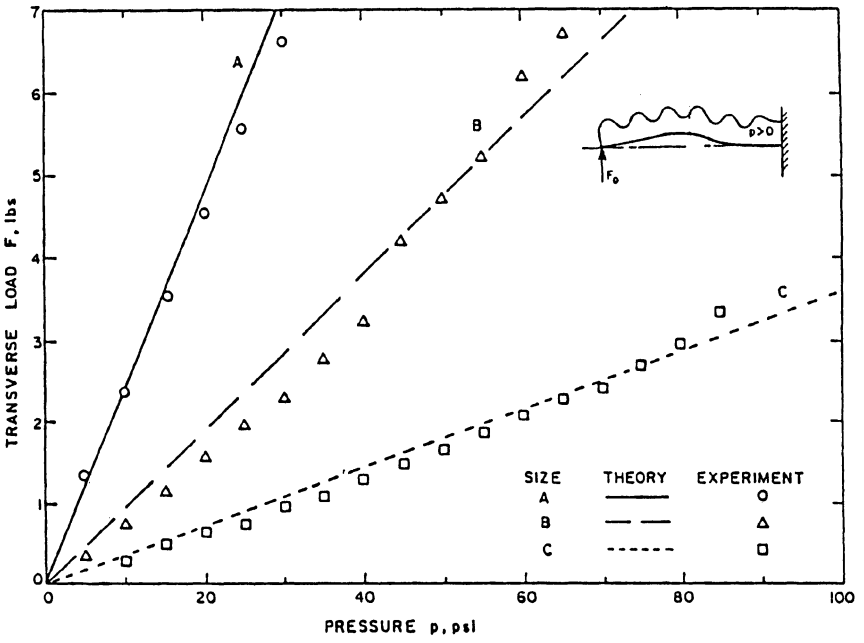

Fig. 5 Transverse tip load required to supress tip displacement for pressurized, polyurethane elements A, B, and C.

1. Flexible Robotic Arm Manipulator

The counterpart of the elephant trunk, or the arm manipulator and its end effector (gripper), are shown in Fig. 6. This system, discussed in detail by Wilson (1987), consists of software Programs I and II used for open loop control of the arm and gripper. The basic system design is outlined now.

Mechanical Design

The arm manipulator, Fig. 6, is designed from the three different sizes of polyurethane elements listed in the table insert of Fig. 2. The letters A, B, C designate the size and the numbers after these letters designate the element position in the arm. This arm resembles somewhat the trunk of an elephant in both its out-

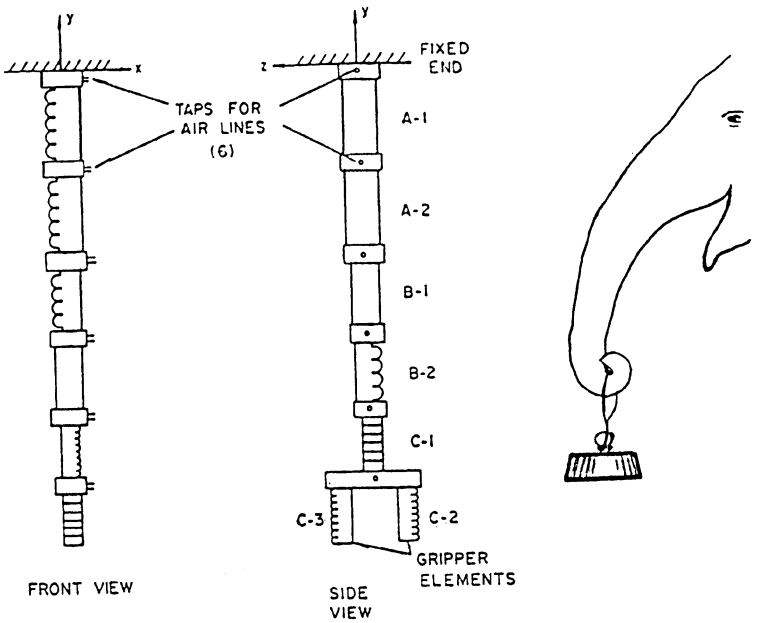

Fig. 6 Flexible arm and gripper, counterpart to the elephant trunk.

ward form and manipulative function and hangs vertically when unpressurized and at rest. The largest elements A-1 and A-2 are at the base and sustain the highest arm moments when the pressurized arm with the payload at the gripper is displaced from the vertical equlibrium position. In terms of the Cartesian coordinate system defined in Fig. 6, arm elements A-1, A-2, B-1, and C-1 are aligned to bend in the x,y-plane; but element B-2 is aligned to bend in the y,z-plane. The latter element is effective in avoiding collisions of the arm with obstacles in the x,y-plane. As discussed below, each arm element is a distinct pressure cell and has its own air supply line connected to the control module. The two opposing elements of the gripper, however, have a common air supply.

Hardware Control System

Shown in Fig. 7a and 7b, respectively, are the fluid circuit and electronic circuit for a single tube element. Each fluid circuit

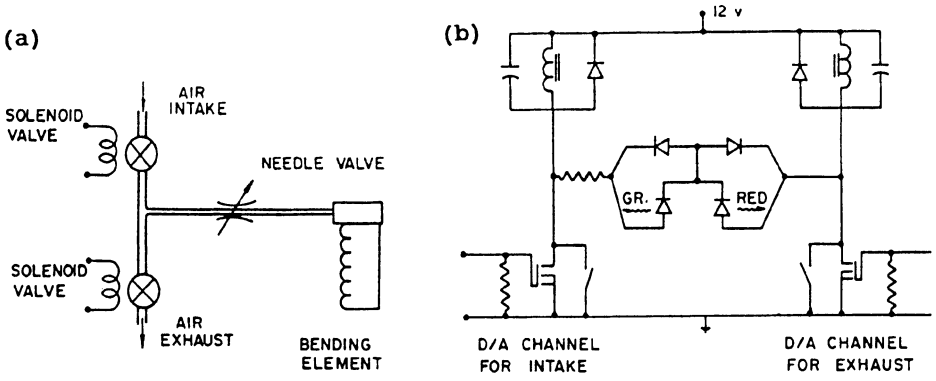

Fig. 7 Circuits for open loop control of a single element: (a) Fluid circuit, (b) Electronic circuit for D/A control of air intake, exhaust.

has two solenoid valves, one for air admission and one for air exhaust, and a hand adjustable needle valve to slow the flow of air, if necessary. Each electronic circuit has two digital channels, one for air admission and one for air exhaust. The system control module consists of six dual units of Fig. 7, one unit for each of the five arm elements and one for the gripper. For arm elements, the admitted air is provided from a 275 kPa regulated source; and for the gripper, air is provided from a 480 kPa regulated source to assure adequate force to grip the payload.

The interface between the system control module and the microcomputer was accomplished with logic-level MOSFET (metal-oxide-semiconductor field-effect transistor) power switches capable of passing the current required by the solenoid valves and of withstanding the voltage surges at solenoid turn-off. Each solenoid was provided with a diode and a capacitor to limit the voltage surge. For control, logic-level MOSFETs accepted signal voltages available from the computer. Logic 0 (0 volts) produced a switch-open effect, and logic 1 (3.5 to 5 volts) produced a switch-closed effect. The interface was designed to operate with a microcomputer through a 8255 parallel output device which was a Techmar Lab Tender board in an IBM-pc-XT.

Two Software Control Methods

Tests of the solenoid valves and the individual bending elements defined in Fig. 2 showed sufficiently small response times for achieving reasonably fast action of the manipulator arm and gripper: 12 msec for the solenoids, 1 sec for the largest bending element A to achieve a 90 deg bend, and 0.3 sec response time for elements B and C.

Tempered with a knowledge of these response times, we developed two open-loop software control methods to achieve pick-and-place arm maneuvers. The first method employs Program I, a timed sequencing method involving incrementing or decrementing the air pressure in each element. For example, Fig. 8 depicts the time sequences during which the intake and exhaust solenoid valves are open to drive the bending elements. The mathematical description of valve operation is a sequence of step functions to open, each followed after some time by a step to close.

The second method employs Program II, or a pressure pulsing method. Figure 9 depicts the control signal for an intake or exhaust solenoid valve in which the valve is open during the pulse width time T1 and closed during the pulse gap time T2. Here, the desired arm and gripper motion is achieved by selecting the pulse width, the pulse gap, and the number of pulses of each solenoid.

Experiments and Discussion of Results

A typical pick-and-place maneuver was chosen to evaluate arm performance, and especially to determine the shortest possible cycle times consistent with both smooth arm motion and a minimum overshoot of the target point and final rest point. Stroboscopic views of an arm and gripper for a typical experiment are shown in Fig. 10. Here, the gripper is pressurized and grasps an object from the lower platform; the arm elements are selectively pressurized to lift the object to an upper platform while avoiding a collision with it; the gripper is depressurized and the object is released; the arm elements are repressurized to raise the arm somewhat; and then all elements are depressurized as the manipulator returns to its initial vertical equlibrium position.

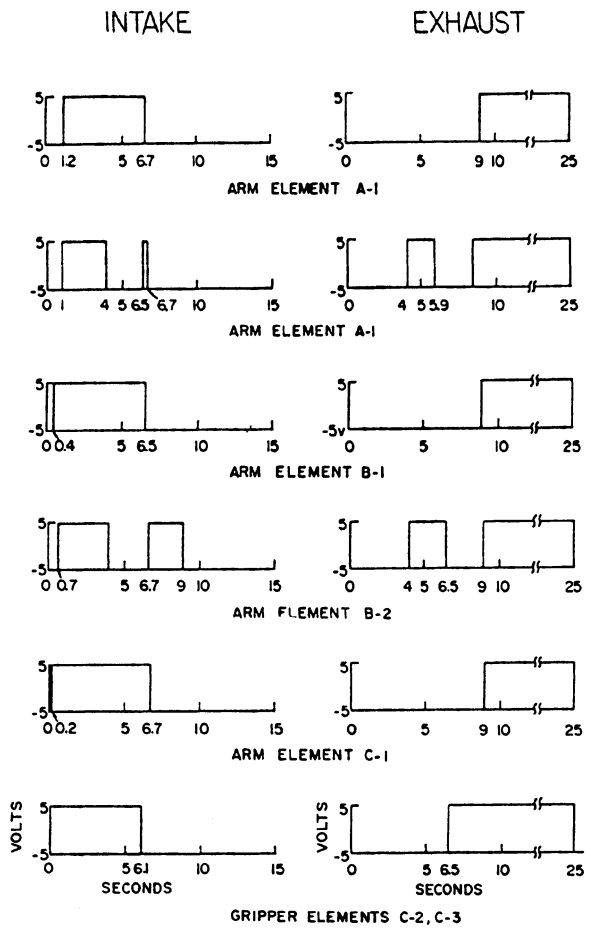

Fig. 8 Timed sequencing for a typical arm maneuver.

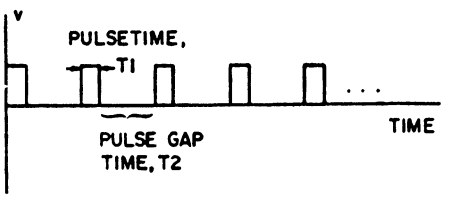

Fig. 9 Definition of the control signal for the pulsing method.

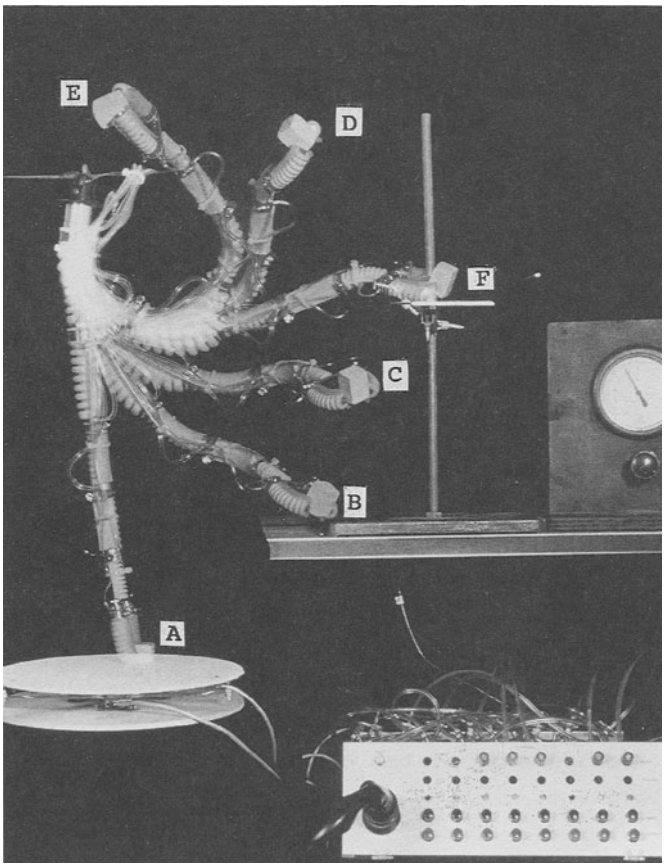

Fig. 10 Stroboscopic photographs for a pick-and-place maneuver: A is the pickup point; B, C, D, and E follow; and F is the placement point for the block on the upper platform. (Photograph by Anthony Benson, courtesy of Scientific American)

The coordinate system of the arm's work space for our series of experiments is defined in Fig. 11. In all experiments, our manuevered object was a wood cube with an edge dimension of 2.54 cm, initially oriented with its sides parallel to the coordinate planes, with its cg located at position X = Y = Z = 0. After the gripper grasped the cube from this location on the lower platform, the arm deposited the cube at the target point on the upper platform, position X = 47 cm, Y = 49 cm, and Z = 5 cm, and the arm returned to its initial vertical position. The total time

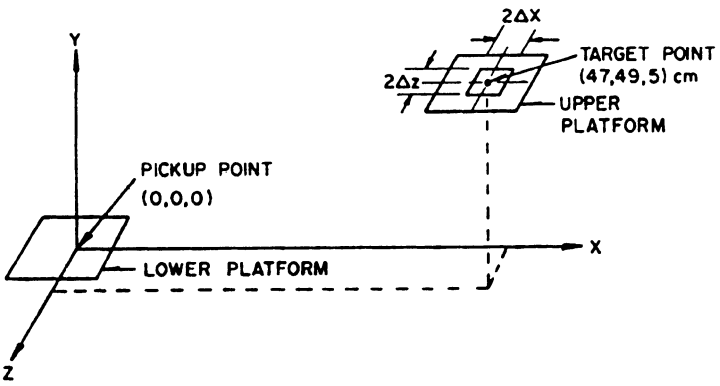

Fig. 11 Coordinate system for the pick-and-place maneuver.

for this maneuver is defined as the cycle time T.

We evaluated the performance of the manipulator and the two control methods several ways: qualitative observations of the smoothness of arm motion; quantitative data on the amplitude and frequency of arm motion at the end of the maneuver; measurements of the deviations ΔX, ΔY, ΔZ from their respective target points; and the change in rotation $\Delta\theta$ of the cube about the Y-axis, from before to after placement.

In the first series of experiments, we employed Program I, the timed sequencing control method with the pressure patterns of Fig 8. We needed to perform several experiments to determine the needle valve settings that minimized unwanted arm oscillations. Qualitative observations of these experiments are summarized as follows. The smoothest arm motion occurred when the needle valves were set to greatly restrict flow of air and where the maneuver cycle times T were 25 seconds. As the needle valves were opened to allow for higher air flow rates, the arm moved faster, and values of T as low as 5 seconds could be achieved. However, we achieved this fast action only at the expense of increased arm oscillations during and immediately after the maneuver cycle.

By contrast, we found that Program II gave superior performance. When we set the needle valves to the fully open position and employed the pulsing control method of Fig. 9, the arm action

was as smooth at cycle times of 5 sec as for the timed sequencing control method at a 25 sec cycle time.

Typical experimental results showing the accuracy of object placement for the pick-and-place maneuver are summarized in Table 1. For both Programs I and II, the time intervals for the maneuver cycle, the pulse, and the gap were fixed. For each program, the change in the object rotation θ and the deviations X and Z from the object's target values were measured in repeated trials. Table 1 gives the maximum measured θ and the maximum percent deviation from the target coordinates, based on 10 trials for each program. The right-most column lists the maximum amplitudes A of free oscillations that occur at the end of the cycles where the arm is depressurized and then swings about its vertical equilibrium position.

The experimental results for the two methods of arm motion control are compared and summarized as follows.

1. If the gap time interval T2 is chosen as zero for pulsing control, Program II of Table 1, then the two control methods are the same.

2. Both control methods may be used successfully for pick-and-place manipulation cycle times T as small as 4.2 seconds.

3. Pulsing is superior to timed sequencing because the pulsing method affords more versatile programming and gives smoother arm motion at a fixed T.

4. The object positioning errors for X and Z were at most 9% for T2 = 0 and T = 4.2 sec. However, these errors decreased when both T2 and T were increased.

5. Object rotations $\Delta\theta$ up to 22 deg were performed.

6. The amplitude A of the end-cycle, free swinging oscillations were at most 7 cm, but this value decreased when both T2 and T were increased.

An increase in object placement accuracy and a decrease in end cycle oscillations may be effected by introducing positioning feedback and damping in the control system. However, the present new-concept manipulator arm with its pulsing, open-loop control method may be used in applications where high accuracy of object placement is not a requirement; and where fast-acting, lightweight, robust, and relatively simple arm structures are needed.

2. Flexible Gripper

Shown in Fig. 12 are a two-fingered gripper and a squid whose tentacles are grasping a shrimp. There is a resemblence in the motion of the experimental gripper and that of the tentacles. The two fingers of our gripper were type B polyurethane tube elements of Fig. 2. With the aid of a force sensor at the base of the gripper, a pressure module, a microcomputer, and interface equipment, we implemented the closed-loop control system (two types) so that the fingers could maintain the gripping force even as arbitrary side loads were applied to one of the fingers. The essential features of this design are summarized as follows.

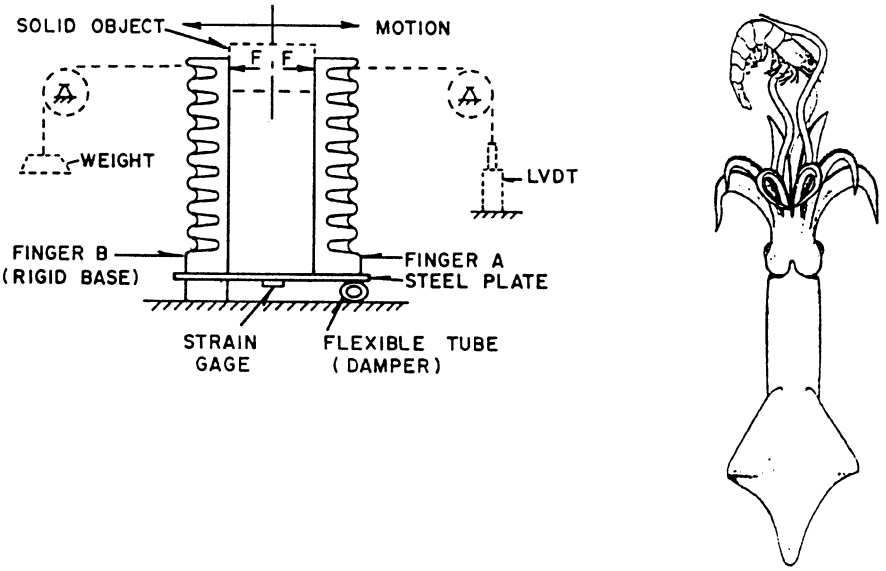

Fig. 12 Mechanical design of the controlled gripper made of two polyurethane elements B, counterpart to a pair of squid tentacles gripping a shrimp. (Squid picture adapted from a photograph by Kier and Smith, 1985).

Mechanical Design

As shown in Fig. 12, a finger is mounted at each end of a relatively stiff plate of spring steel. The transverse gripping force F at a fixed position L on each finger produces a uniform bending moment of magnitude L·F in the plate and a corresponding strain ϵ that varies linearly with F. The soft plastic tube under the plate at finger A serves as a hinge support, provides damping, and effects a sufficiently high natural frequency of 25 hz for this mechanical assembly, well above the 6 hz resonance measured for the electronic circuit/pneumatic valve system described presently.

As each finger is pressurized, it bends inward to clamp the solid object at a predetermined gripping force F and the plate strain ϵ is measured. The strain sensor is a foil-type strain gage that forms one arm of a Wheatstone bridge circuit, where the unbalance of the bridge voltage, measured through an appropriate signal conditioner, gives a measure of ϵ. As the fingers manipulate the gripped object in a prescribed way, the air pressure in each finger is regulated so that ϵ remains constant, or nearly so. In this way, the fingers' gripping force remains essentially constant even when external side loads are applied, as shown by the broken lines of Fig. 12. The linear variable differential transformer (LVDT) shown in this figure is used to measure the horizontal displacement of the fingers, but is not a part of the finger manipulation and control system.

Control System and Computer Interface

Two control systems were developed. Control Method 1, shown in Fig. 13a, provides force control through the first servovalve which sets the internal air pressure. Relative finger movements are controlled by the second servovalve, the positioning valve. Control Method 2, shown in Fig. 13b, employs one servovalve per finger. Finger A movement is set by computer control and Finger B is moved under computer control to maintain the desired clamping force. This is done through feedback from the strain gage.

Each control system provides accurate control of the gripping force and the horizontal finger position. Each system uses

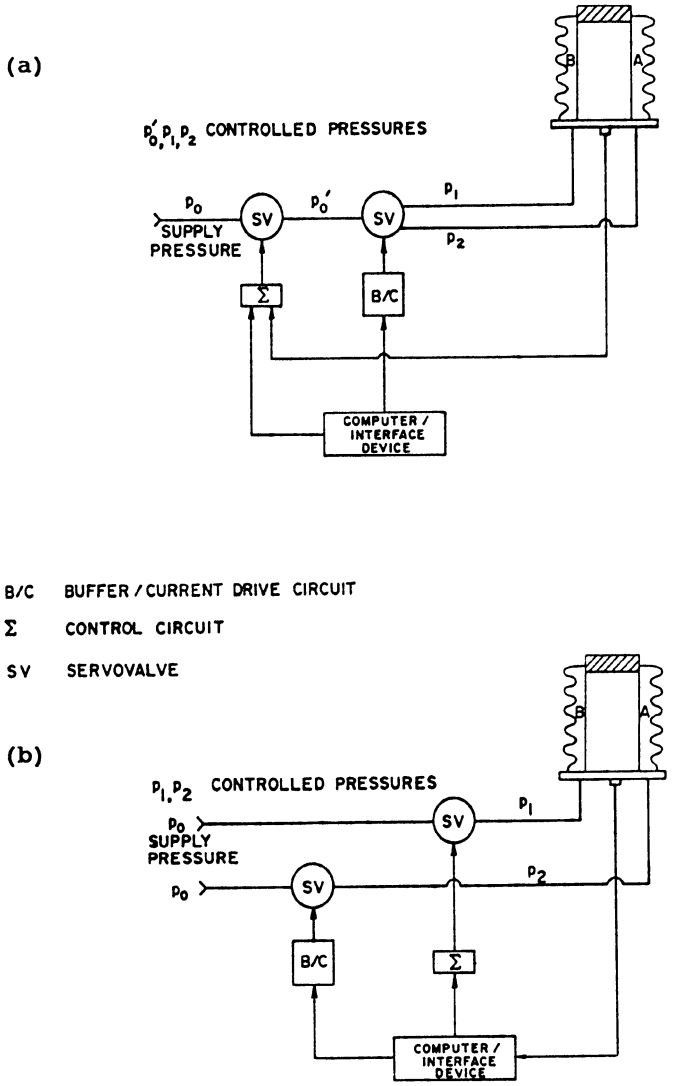

Fig. 13 Control systems for two-fingered gripper experiments: (a) Control Method 1, (b) Control Method 2. Servovalves: No. 200 PN, Atchley Controls, Los Angeles, CA.

a microcomputer for finger control and a monitor displays the dynamic gripping force. Analog inputs for the feedback controlled gripper force are the strain gage voltage and the reference voltage proportional to the preset gripper force F. The reference voltage is obtained from an Apple II computer output port.

An interface, an ISAAC 91A, was added to the Apple II computer to handle the analog input and output signals. Differential buffer circuits follow the interface outputs for signal gain and thereby increased the capability for sourcing/sinking current of + 20 mA. Strain gage sensing provides a negative feedback voltage to maintain the desired gripping force.

The system response time is limited by its mechanical resonance frequency of 25 Hz. An increase in the feedback system gain decreases the response time and increases overshoot. Practical settings are: 0 to 5 V for strain gage input; -5 to +5 V for the computer/interface outputs; and a buffer gain of 33 to allow for quick response time without exciting resonance behavior. Undesirably large signals are controlled by Zener diodes in the buffer circuit. Details of the circuit designs and printouts of the the control software are given by Wilson (1984b).

Experiments and Discussion of Results

The two-fingered gripper was evaluated in a series of ex-experiments, eight of which are presented herein. The purposes of these experiments were: to compare the response times and accuracy o f the two control systems; to measure reproducibility of finger displacement; and to measure how well the fingers could maintain a constant gripping force on an object, both with and without horizontal side loads applied to each finger.

In each of these eight experiments, the fingers were programmed to grip a block of wood of dimensions 2.54 by 5 by 5 cm with a preset force F of 8.1 N, and to move this block side to side with nearly harmonic displacement amplitudes of + 1.9 cm. Listed on the left side of Table 2 are the sets of different conditions imposed for each experiment: the cycle times of 1.6 or 2 sec, and the horizontal side loads (see Fig 12) of 0, 1.42 N, or 0.86 N.

The experimental results for the two methods of gripping are summarized and compared as follows. See the right side of Table 2 for measured values of gripping force.

1. In the absence of horizontal side loads on Fingers A and B, there was very little difference in the accuracy with which

these two control systems maintained the prescribed value of F: within 1.8% for Method 1 and within 2% for Method 2. This was true for both the faster motion (1.6 sec cycle time) and the slower motion (2 sec cycle time).

2. When horizontal side loads were added to each finger, for both control methods the 1.6 sec cycle time led to an overshoot in F; but this overshoot was less severe for Method 1 (16.7%) than for Method 2 (25.6%).

3. The time during which F exceeded 2% of its prescribed value was always less than 10% of its cycle time.

4. When the cycle time was increased to 2 sec (or longer, as indicated by other experiments), the effects of added side loads disappeared, and the accuracy required to maintain F was that of zero side load.

Not included in these eight experiments are those on repeatability, or the ability of the finger tip to return to an original horizontal position under the original set of internal finger pressures, while maintaining a constant gripping force. Results of these experiments show a maximum deviation of + 11% in the horizontal tip deflection δ between δ measured for a set of finger pressures as pressure increased, and δ measured for the same set of finger pressures as pressure decreased. Such deviations between loading and unloading cycles show the effects of material hysteresis which is always apparent to some degree in polymeric materials such as polyurethane.

From this two-part study, we conclude that the flexible arm manipulators and grippers are fast-acting, robust, and practical. Typical laboratory-scale versions have ratios of payload to self-weight in the range from one to five. On a larger scale, two-fingered grippers resemble a pair of controlled arm manipulators or tentacles and may be useful in construction projects, for in-instance, for gripping and manipulating objects too heavy for humans to handle.

Acknowledgements

Part 1 was sponsored in part by the U.S. Defense Advanced Research Projects Agency under Contract No. MDA903-84-C-0243 to

Duke University. Part 2 was sponsored in part by Lord Corporation under a consulting contract to the senior author. The authors appreciate the experimental assistance of Richard Lazarus and Glenn Butcher; and thank Jack Rebman, project monitor of Lord Corporation, for suggesting the two-fingered gripper design.

Table 1 Typical Experimental Results for Placement Accuracy of the Manipulator Arm

PROG.	T sec	T1 ms	T2 ms	ΔX mm	ΔY mm	ΔX/X ×100%	ΔY/Y ×100%	Δθ deg	A cm
I	16.4	70	210	+2	+2.5	+0.43	+5	22	4
II	4.2	105	0	+4	+4.5	+0.85	+9	15	7

Table 2 Typical Experimental Results for a Two-Fingered Gripper in Harmonic Motion While Grasping a Block

Imposed Conditions (block displacement: ±1.9 cm)			Measured Gripping Force F (N)	
Cycle Time (sec)	Side Load (N) Finger A	Finger B	Control System 1	Control System 2
1.6	0	0	8.1±0.14	8.1±0.16
2	0	0	8.1±0.14	8.1±0.16
1.6	1.42	0.86	8.1±1.35	8.1±2.07
2	1.42	0.86	8.1±0.14	8.1±0.16

References

1. Backe, W. The application of servopneumatic drives for flexible mechanical handling techniques. Robotics and Autonomous Systems. Vol 2, pp. 45-56. 1986

2. Cutkowsky, M. R. Mechanical properties for the grasp of a robotic hand. Report No. CMU-RI-TR-84-24, Robotics Institute, Carnegie-Mellon Univ. Pittsburgh, Pa. 1984
3. Dario, P. and Buttazzo, G. An anthropomorphic robot finger for investigating artificial tactile perception. Int. J. of Robotics Res. Vol. 6, pp. 25-48. 1987
4. Datseris, P. and Palm, W. Principles on the development of mechanical hands which can manipulate objects by means of active control. ASME paper No. 84-DET-37. 1984
5. Ghattas, G. Mechanics of flexible, pneumatic structural elements for robotic limbs. MS Thesis, Duke U., Durham, NC. 1988
6. Hanafusa, H. and Asada, H. Stable prehension by robot hand with elastic fingers. Proc. 7th Int. Symp. Indus. Robots. Tokyo. 1977
7. Iberall, T. The nature of human prehension: three dextrous hands in one. IEEE Int. Conference on Robotics and Automation Vol.1, pp. 396-401. 1987
8. Jacobson, S. C., Wood, J. E., Knutti, D.F., and Biggers, K. B. The Utah/ MIT dextrous hand: work in progress. Int J. of Robotics Res. Vol. 3 pp. 21-50. 1984
9. Kerr, J. and Roth, B. Analysis of multifingered hands. Int. J. of Robotics Res. Vol. 4, pp. 3-17. 1986
10. Kier, W. M. and Smith, K. K. Tongues, tentacles and trunks: biomechanics of movement in muscular hydrostats. Zool. J. Linnaen Soc. Vol. 83 pp. 307-324. 1985
11. Kumar, V. and Waldron, K. J. Suboptimal algorithms for force distribution in multifingered grippers. IEEE Int. Conf. on Robotics and Automation Vol. 1, pp. 252-257. 1987
12. Lee, J. Kinematic synthesis of industrial robot hand/gripper -a creative design approach. Robots and Autonomous Systems. Vol. 4, pp. 257-263. 1988
13. Li, Z. and Sastry, S. Task oriented grasping by multi-fingered robot hands. IEEE Int. Conf. on Robotics and Automation. Vol. 1, pp. 389-394. 1987
14. Nguyen, Van-Duc. Constructing stable grasps. Int. J.of Robotics Res. Vol. 8, pp. 26-37. 1989
15. Palaniappan, M. Large deflections of continuous elastic structures. MS Thesis, Duke Univ., Durham, NC. 1986
16. Salisbury, J. K. and Craig, J.J. 1982. Articulated hands: force control and kinematic issues. Int. J. of Robotics Res. Vol. 1. 1982
17. Snyder, J. M. and Wilson, J. F. Dynamics of the elastica with end mass and follower loading. J. Appl. Mech. Vol 56, 1990
18. Wilson, J. F. Robotic mechanics and animal morphology. Robotics and Artificial Intelligence, M. Brady et al, eds., Springer-Verlag, NY. pp. 419-443. 1984a
19. Wilson, J. F. Active control of a two-finger manipulator. Lord Corp. Report, School of Engineering, Duke Univ. Durham, NC. 1984b
20. Wilson, J.F. Compliant robotic structures, Part III. U.S. Dept. of Defense, ADA192426, NTIS, Springfield, VA. 1987
21. Wilson, J.F. and Mahajan, U. The mechanics and positioning of highly flexible manipulator limbs. J. Mechanisms, Transmissions, and Automation in Design. Vol.111, pp. 232-237. 1989
22. Wilson, J.F. and Snyder, J. M. The elastica with endload flip over. J. Appl. Mech. Vol. 55, pp. 845-848. 1988